RSC Advances

PAPER

View Article Online
View Journal | View Issue



Cite this: *RSC Adv.*, 2017, **7**, 47177

# Theoretical design of a surface plasmon resonance sensor with high sensitivity and high resolution based on graphene–$WS_2$ hybrid nanostructures and Au–Ag bimetallic film

Minghong Wang,[a] Yanyan Huo,*[a] Shouzhen Jiang,[a] Chao Zhang,[a] Cheng Yang,[a] Tingyin Ning,[a] Xiaoyun Liu,[b] Chonghui Li,[a] Wenyuan Zhang[a] and Baoyuan Man[a]

Received 29th July 2017
Accepted 2nd October 2017

DOI: 10.1039/c7ra08380g

rsc.li/rsc-advances

We proposed a high sensitivity and a high resolution surface plasmon resonance sensor composed of graphene–$WS_2$ hybrid nanostructure and Au–Ag bimetallic-layers film. The bimetallic-layer configuration uses the high sensitivity of gold and the narrow full width at half maximum (FWHM) of silver to improve the sensor's sensitivity and resolution respectively. Graphene and $WS_2$ serve as an effective light absorption medium. Once they cover the bimetallic-layer, the sensitivity can be further improved significantly. Graphene–$WS_2$–Au–Ag model shows a higher sensitivity and higher resolution than that of the conventional sensing scheme where pure Au thin film is used. In our paper, we mainly use Fresnel equations and the transfer matrix method (TMM) to study the reflectivity and sensitivity as well as the full width at half maximum (FWHM) of the SPR sensor.



## 1. Introduction

Surface plasmon resonance (SPR) sensors have become an important sensing technology in the field of biology and chemistry because of their extraordinary high sensitivity, biocompatibility, detection accuracy, *etc.*[1–4] In general, there are two common detection methods used for SPR sensors based on Kretschmann configuration, including wavelength interrogation and angle interrogation. For wavelength interrogation, polychromatic light is required as the incident light. However, for angle interrogation, only monochromatic light is required, it is possible to achieve higher signal-to-noise ratio due to the wavelength and power stability of the source.[5–11] Thus, angle interrogation is adopted in this article.

Gold, silver, or bimetallic (Au–Ag) films are usually used as the sensor-layer in the traditional SPR sensor. The sensitivity of the Au film SPR sensor is highest but the resolution is lowest of these three metallic film. The SPR sensor based on Ag film has the highest resolution, but the sensitivity is relatively low. The bimetallic film can improve the resolution of the SPR sensors, but the sensitivity will be reduced.[12–15] In addition, the metal based on a SPR sensing layer is unstable and easily oxidized, further limiting its application. Therefore, how to give consideration to both sensitivity and resolution is crucial to obtain a SPR sensor with excellent behaviors.

Graphene was discovered first in 2004 has attracted great attention in recent years, due to its compelling unique electrical and optical properties.[16–20] Once graphene is deposited on metallic thin films, the sensitivity of the SPR sensor can be enhanced.[21] However, the sensitivity of these SPR sensors was only enhanced by 25% when ten layers graphene were coated on the Au film.[22] The enhanced effect of single nanomaterial toppings still seems insufficient for SPR biosensor applications. Afterwards, two layers of nanomaterials such as silicon–graphene, silicon–$WS_2$ and $MoS_2$–graphene hybrid nanostructures were studied to enhance the sensitivity.[23,24] The sensitivity of the SPR sensor based on two layers of nanomaterials can be effectively enhanced, but the FWHM also increased significantly, which leads to a lower resolution.[25]

In this paper, we design a new sensing configuration composed of graphene, $WS_2$ nanomaterials and Au–Ag bimetallic-layer, which has a higher sensitivity and a higher resolution. Au–Ag bimetallic layer is used to reduce the full width at half maximum (FWHM). Graphene and $WS_2$ can improve the light absorption, which is much beneficial for obtaining of the SPR signal with high sensitivity. In addition, graphene layer has a large specific surface area and can selectively detect aromatic compounds through pi-stacking fore. The sensitivity and the FWHM of SPR sensor are systematically studied by using Fresnel equations and the transfer matrix method.

[a]*School of Physics and Electronics, Shandong Normal University, Jinan 250014, China. E-mail: yanyanhuo2014@sdnu.edu.cn*

[b]*Institute of Electronic Science and Technology, Xi'an Jiaotong University, Xian 710000, China*

## 2. Theory

The SPR sensor proposed in this paper is based on the Kretschmann configuration, as shown in Fig. 1. The first layer is the SF11 prism and its refractive index is $n_1 = 1.52$.[25] The second layer is Ag film and the third layer is Au film. The complex refractive index of thin-metal is obtained from the eqn (1) at 633 nm.[26]

$$\varepsilon = \varepsilon_r + i\varepsilon_i = \left(1 - \frac{\lambda^2\lambda_c}{\lambda_p{}^2(\lambda_c + i\lambda)}\right) \quad (1)$$

where, $\lambda_p$ and $\lambda_c$ represent the plasma and the collision wavelengths of the metals, respectively. The dielectric constant of Ag and Au at 633 nm are $\varepsilon_{Ag} = -17.81 + i0.68$ and $\varepsilon_{Au} = -10.98 + i1.46$ respectively. Next layer is $WS_2$ or $MoS_2$ and their dielectric constant are $\varepsilon_{WS_2} = 23.85 + i3.06$ and $\varepsilon_{MoS_2} = 24.44 + i11.91$ at 633 nm.[27] The fifth layer is graphene and its complex refractive index is obtained from the eqn (2) at 633 nm.[25]

$$n = 3.0 + i\frac{C_1}{3}\lambda \quad (2)$$

where $C_1 \approx 5.446\ \mu m^{-1}$. The last layer is biomolecular analyte, which is replaced by the deionized (DI) water firstly and its refractive is $n_6 = 1.332$.

We use the transfer matrix method (TMM) and the Fresnel equation to analyze the reflectivity and FWMH of the sensor based on graphene–$WS_2$–Au–Ag hybrid nanostructure. In N-layer model, the tangential field components at the first and the last interface are related as:[25]

$$\begin{bmatrix} U_1 \\ V_1 \end{bmatrix} = M \begin{bmatrix} U_{N-1} \\ V_{N-1} \end{bmatrix} \quad (3)$$

where, $U_1$ and $U_{N-1}$ are the tangential component of electric field of the first layer and the last layer, $V_1$ and $V_{N-1}$ are the tangential component of magnetic field of the first layer and the last layer. $M$ is the characteristic Transfer Matrix (TM) of the combined N-layer structure and can be obtained from the following relation for the p-polarization light

$$M = \prod_{k=2}^{N=1} M_k = \begin{bmatrix} M_{11} & M_{12} \\ M_{21} & M_{22} \end{bmatrix} \quad (4)$$

where

$$M_k = \begin{bmatrix} \cos\alpha_k & (-i\sin\alpha_k)/\chi_k \\ -i\chi_k \sin\alpha_k & \cos\alpha_k \end{bmatrix} \quad (5)$$

and

$$\chi_k = \left(\frac{\mu_k}{\varepsilon_k}\right)^{1/2} \cos\theta_k = \frac{\left(\varepsilon_k - {n_1}^2 \sin^2\theta_1\right)^{1/2}}{\varepsilon_k} \quad (6)$$

$$\alpha_k = \frac{2\pi}{\lambda} n_k \cos\theta_k (Z_k - Z_{k-1}) = \frac{2\pi d_k}{\lambda}\left(\varepsilon_k - {n_1}^2 \sin^2\theta_1\right)^{1/2} \quad (7)$$

$\varepsilon_k$ and $d_k$ are the dielectric constant and thickness of the $k_{th}$ layer, $\theta_1$ and $\lambda$ are the incident angle and the wavelength of the incident light. The total reflection coefficient ($r_p$) for the p-polarization light is

$$r_p = \frac{(M_{11} + M_{12}\chi_N)\chi_1 - (M_{21} + M_{22}\chi_N)}{(M_{11} + M_{12}\chi_N)\chi_1 + (M_{21} + M_{22}\chi_N)} \quad (8)$$

The reflectivity ($R$) of the configuration for p-polarization light are obtained as

$$R = |r_p|^2 \quad (9)$$

The curve of the reflectivity ($R$) changed as the incident angle ($\theta_1$) is called SPR curve. The resonant angle ($\theta_{SPR}$) is the angle corresponding to the minimum reflectivity ($R_c$), which will shift with the varied refractive index of the sensing layer induced by the binding of the analyte. The sensitivity of a SPR sensor is defined as:

$$S(\theta) = \frac{\Delta\theta}{\Delta n} = \frac{d\theta}{dn} \quad (10)$$

$\Delta\theta$, $\Delta n$ are the variation of resonance angle and refractive index of the sample.

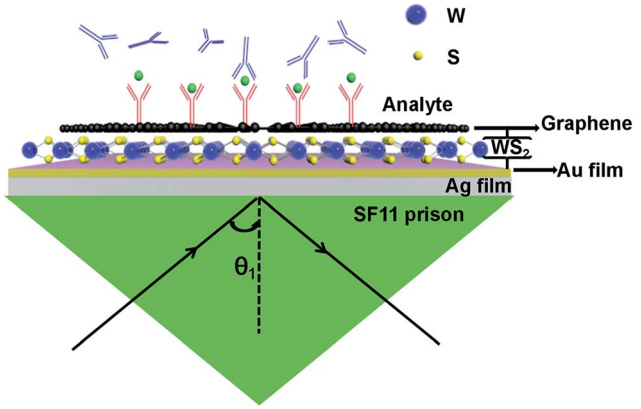


Fig. 1 A schematic diagram of the SPR sensor system.

## 3. Results and discussions

According to principle of energy conservation: when the reflectivity reaches the minimum value, the maximum energy from the incident light can be coupled to the surface plasmon, which can enhance the sensitivity and resolution of a SPR sensor.[28–30] Thus, the optimum thickness can be found based on principle of energy conservation. Fig. 2(a) shows that the minimum reflectivity $R_c$ at the resonant angle $\theta_{SPR}$ of the gold–silver bimetallic film SPR sensor changed as the thicknesses of silver and gold layer. The minimum value of $R_c$ can be very close to 0 when the gold and silver layers take appropriate thicknesses, which corresponding to the optimized thicknesses of silver and gold film. The optimized thickness values of the gold and silver layers are shown in Fig. 2(b). We find that the thickness of one metal layer decreases with increasing thickness of the another metal layer for the optimized thicknesses of the bimetallic layer. When the thickness of Ag layer increases to 52 nm, the corresponding thickness of Au layer is 0 nm. While as the thickness of Au layer

 

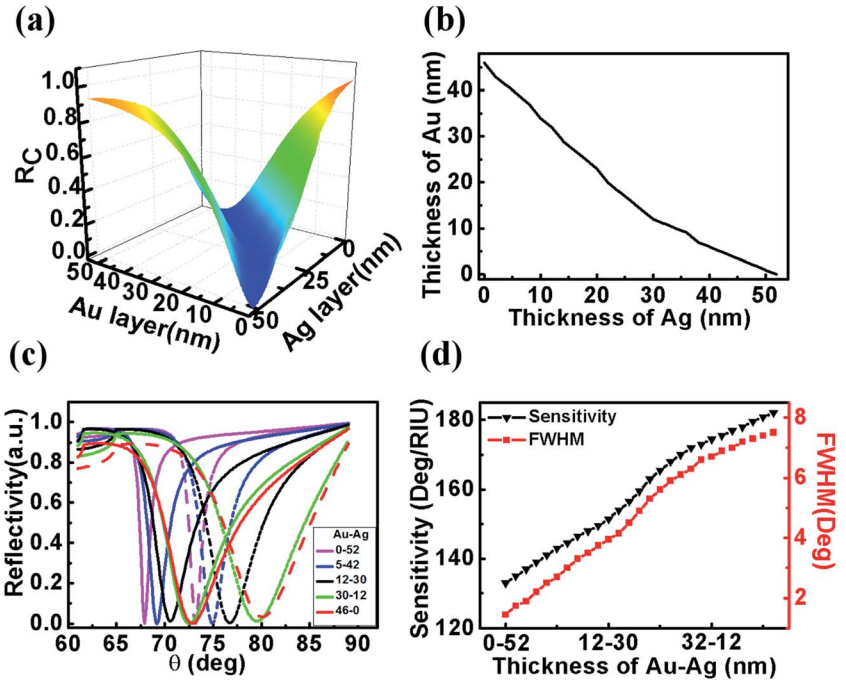


Fig. 2 (a) Reflectivity ($R_c$) at resonance angle with various thicknesses of silver and gold film. (b) The optimized thicknesses of Au–Ag bimetallic layer in the bimetallic film SPR sensor that achieve minimal reflectivity at resonance angle. (c) Reflectivity curves of Au–Ag layer with different optimized thickness *versus* the angle of incidence. Solid lines and dashed lines depict the reflectivity curve corresponding the analyte refractive index of 1.332 and 1.372, respectively. (d) Sensitivity and FWHM of SPR sensor with varying Au–Ag optimized thicknesses.

increases to 46 nm, the corresponding thickness of Ag layer is 0 nm. So the calculating thickness range of gold and silver layer are 0–46 nm and 0–52 nm respectively.

The sensitivity and FWHM of SPR sensor with the optimized thicknesses of bimetallic layer are calculated in Fig. 2(c) and (d). From Fig. 2(c), we can see that the resonance angle and FWHM of the bimetallic film SPR sensor are different for different optimized thicknesses of Au–Ag bimetallic layer. When the thickness of Ag and Au are 52 nm and 0 nm, *i.e.* only Ag film on the SF11 prison, the resonant angles is 67.9 Deg, and the FWHM is only 1.5 Deg. While there is only Au film on the SF11 prison, the resonant angles is 72.8 Deg, and the FWHM is 7.5 Deg. The sensitivities of sensor based on pure Ag and Au film are 133 and 182 Deg per RIU, which are obtained by changing the refractive index of analyte by $\Delta n = 0.04$. From the results, we know that the sensitivity of sensor for pure Au film is higher than that of pure Ag film, but the FWHM of sensor for pure Au film is higher than that of pure Ag film. So the SPR sensor with high sensitivity and high resolution cannot be realized by using only one single metallic film. However, when single metallic film is replaced by bimetallic film, the sensitivity of SPR sensor increases with increasing thickness of Au film, but it decreases with increasing thickness of the Ag film. While the FWHM decreases with increasing thickness of Ag film, but increases with increasing thickness of the Au film, as shown in Fig. 2(d). So, the Au film can improve the sensitivity of the SPR sensor, while the Ag film can improve the resolution. However, for the optimized bimetallic film SPR sensor, although the resolution can be enhanced, the sensitivity is reduced significantly.

Two-dimensional materials not only can improve the sensitivity of a SPR sensor, but also can protect the metal layer from oxidation and enhance the adsorption of biological and chemical molecules.[31–34] Here, we mainly study the performance of sensor when three kinds of two-dimensional materials ($WS_2$, graphene and $MoS_2$) are covered on bimetallic layer.[32–34] To optimize the number of two-dimensional material layers, we plotted the reflectivity curves of the SPR sensor composed of Au–Ag bimetallic film and two dimensional materials with different numbers of layer, as shown in Fig. 3(a–c). The thickness of the silver layer and gold layer are chosen as 30 and 12 nm. As shown in Fig. 3(a–c), when different layers of $WS_2$, graphene and $MoS_2$ are covered on the bimetallic film, some characteristics of the resonant curve are concluded as: (I) the resonant angle shifts to the larger angles with increasing numbers of $WS_2$, graphene and $MoS_2$ layer. For $WS_2$ and $MoS_2$, the shifts of resonance angle are larger than that of graphene, which is caused by the larger real part of the dielectric constant of $MoS_2$ and $WS_2$.[22,24] (II) The FWHM of the SPR curve becomes larger as the numbers of graphene, $MoS_2$ and $WS_2$ layer increase. Especially, for $WS_2$ and $MoS_2$, the FWHMs have a rapid broadening, because of a larger electron energy loss caused by the larger imaginary part of dielectric constant of $WS_2$ and $MoS_2$. (III) The minimal value of reflectivity $R_c$ at the resonant angle appears when monolayer structure is deposited on Au–Ag bimetallic film for these three kinds of two dimensional materials, as shown in Fig. 3(d), which indicates that the light is effectively absorbed and can promote a stronger SPR excitation. So we choose monolayer $WS_2$,

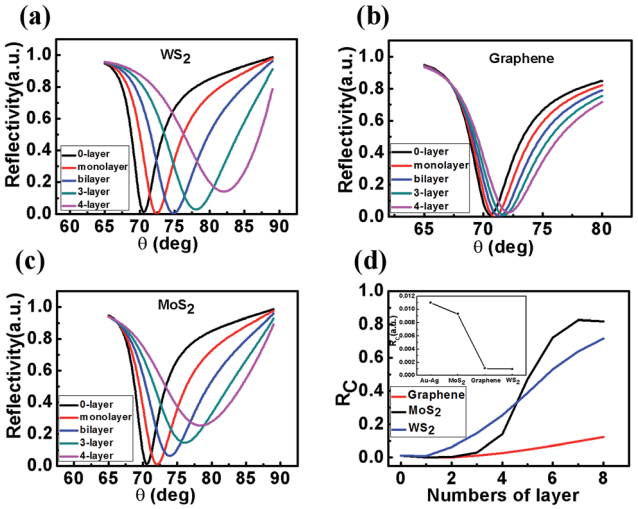


Fig. 3 (a–c) Reflectivity curves of sensor based on bimetallic film and two-dimensional materials with different number of layers for $WS_2$ (a), graphene (b), $MoS_2$ (c), respectively. (d) Reflectivity $R_c$ at resonance angle with varying numbers of graphene, $MoS_2$, and $WS_2$ layer and inset: the values of Min $R_c$ for Au–Ag, Graphene, $MoS_2$ and $WS_2$.

graphene or $MoS_2$ deposited on Au–Ag bimetallic film to make a SPR sensor.

In order to investigate the performance of the SPR sensor with bimetallic layers and single layer two-dimensional material, the sensitivity and FWHM of SPR sensors composed of monolayer $WS_2$, graphene or $MoS_2$ and Au–Ag bimetallic film are shown in Fig. 4. When the refractive index of analyte layer changes from 1.332 to 1.372, the resonant angles shift 6.3, 6.8 and 7.1 Deg for graphene, $MoS_2$ and $WS_2$ SPR sensor, respectively. The sensitivities are calculated to be 157.5, 170.0 and 177.5 Deg per RIU, respectively, which are all higher than that of the sensor composed only Au–Ag bimetallic film (only 151.5 Deg per RIU). Because the sensitivity depends on the evanescent field strength which directly related to the absorbed light energy. From inset of Fig. 3(d), we can see that the Min $R_c$ of the bimetallic sensor based on $WS_2$ is the smallest, which means that $WS_2$ can promote the absorption of light more effectively. So the SPR sensor composed of $WS_2$ and Au–Ag bimetallic film is most sensitive for these three kinds of two-dimensional materials. Comparing with the sensor based on pure Au film, its sensitivity is slightly smaller but the FWHM is only 5.1 Deg, which is much smaller than that of SPR sensor composed of pure Au film. Thus $WS_2$ is the best choice for SPR sensors in these three kinds of two-dimensional materials.

Graphene has many advantages for biosensing applications, especially it can selectively detect aromatic compounds and enhance the sensitivity of sensor. So we deposit graphene on $WS_2$–Au–Ag hybrid nanostructure to form a new SPR sensor. The sensitivity and FWHM of the SPR sensor based on graphene–$WS_2$–Au–Ag hybrid nanostructure are calculated in Fig. 5. When monolayer graphene is deposited on $WS_2$–Au–Ag hybrid nanostructure, the sensitivity is further enhanced, can reach up to 182.5 Deg per RIU which is higher than the SPR sensor based on single $WS_2$ film and others. Because the min $R_c$ of this sensor is only $1.07 \times 10^{-3}$ which is the lowest than others based on single $WS_2$ film and others. So it can further absorb the light and get the highest sensitivity. However, the FWHM is also increase a little (5.4 Deg). When the number of graphene layer continues to increase, the sensitivity increases firstly and then decreases, as shown in Fig. 5(a). When the number of graphene layer is 4, the sensitivity can reach to a maximum value (192.5 Deg per RIU), which is higher than the SPR sensor based on only single Au film. The FWHM (7.3 Deg) is a little smaller than that of sensor based on pure Au film. If the number of graphene layers increase to 5, although the sensitivity is also higher than that pure Au film sensor, the FWHM is larger than that of the pure gold. So we can realize a SPR sensor with a higher sensitivity and a higher resolution than pure Au film sensor by using graphene with less than 4 layers and $WS_2$–Au–Ag hybrid nanostructure.

In the above, we only discuss the sensor based on Au–Ag bimetallic with the thickness of 12 and 30 nm. In Fig. 6, we also discuss the sensitivity and FWHM of the sensor composed of monolayer graphene, monolayer $WS_2$ and Au–Ag bimetallic layer with other optimized thicknesses. The sensitivity and the

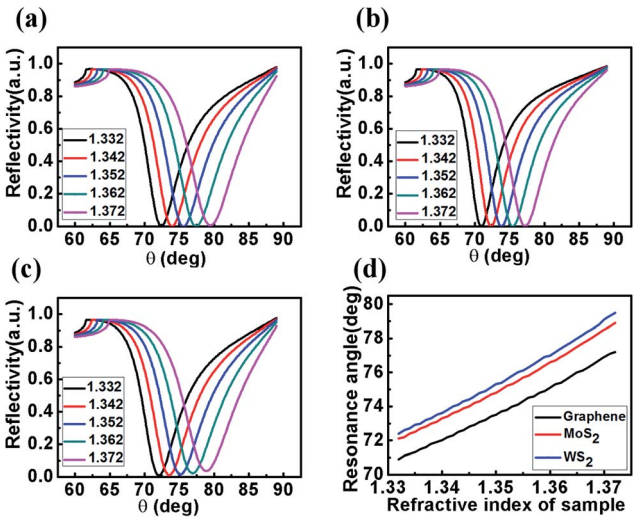


Fig. 4 (a–c) Reflectivity curves of sensors based on bimetallic film and two-dimensional materials as the refractive index of analyte layer changes from 1.332 to 1.372 for $WS_2$ (a), graphene (b), $MoS_2$ (c). (d) Resonance angle of sensors based on bimetallic film and graphene, $MoS_2$ or $WS_2$ film with respect to the refractive index of analyte layer.

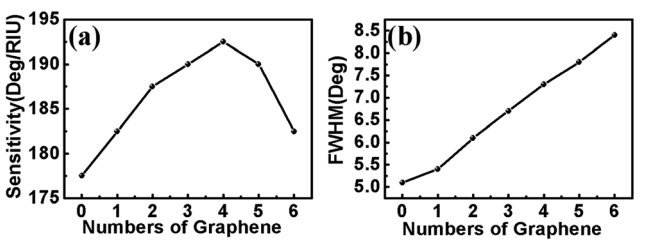


Fig. 5 Sensitivity (a) and FWHM (b) of SPR sensor based on graphene–$WS_2$–Au–Ag film with respect to the numbers of graphene layer.

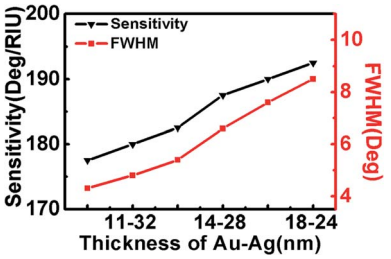


Fig. 6 Sensitivity and FWHM of SPR sensor based on graphene–$WS_2$–Au–Ag film with respect to the different optimized thicknesses of silver–gold bimetallic film.

FWHM decrease gradually as Ag film thickness increases, while increase with increasing thickness of Au film. However, when the optimized thickness of Au–Ag bimetallic layer reach to 16–26 nm, the FWHM of the SPR curve will exceed that of SPR sensor with only single gold film. Similarly, when the optimized thickness of Au–Ag bimetallic layer reach to 11–32 nm, the sensitivity of the SPR sensor will be lower than that of SPR sensor with pure gold film. So if we want to realize a SPR sensor with a higher sensitivity and a higher resolution, the optimized thickness range of Ag and Au layer are 26–32 nm and 11–16 nm respectively.

## 4. Conclusion

In this article, a high sensitivity and resolution SPR sensor is proposed. Based on the Kretschmann configuration, the system consists of graphene, $WS_2$ and Au–Ag bimetallic thin film. In order to obtain a higher sensitivity and resolution sensor, we systematically investigate the optimized thicknesses of Au–Ag bimetallic layer and the optimized layers of 2D nanomaterials. Fresnel equations and transfer matrix method are used to analyze the change of resonance angle, the corresponding sensitivity, and the FWHM for angular modulation of SPR sensor. The result shows that when monolayer graphene and monolayer $WS_2$ are deposited on Au–Ag hybrid nanostructure, the sensitivity can reach up to 182.5 Deg per RIU and the FWHM is only 5.4 Deg, which are superior to the sensor based on only pure Au film. We also discuss the influence of the other optimized thicknesses. If we want to realize a SPR sensor with a higher sensitivity and a higher resolution, the optimized thickness range of Ag and Au layer are 26–32 nm and 11–16 nm respectively.

## Conflicts of interest

There are no conflicts to declare.

## Acknowledgements

The authors are grateful for financial support from the National Natural Science Foundation of China (11504209, 11474187, 11774208, 11404195, 11674199), Shandong Province Natural Science Foundation (ZR2017BA004) and Excellent Young Scholars Research Fund of Shandong Normal University.

## References

1 G. Zheng, Y. Chen, L. Xu and W. Su, *Opt. Lett.*, 2016, **41**, 1582–1585.
2 E. Ozbay, *Science*, 2006, **311**, 189–193.
3 G. Gupta and J. Kondoh, *Sens. Actuators, B*, 2007, **122**, 381–388.
4 S. K. Srivastava, R. Verma and B. D. Gupta, *Opt. Commun.*, 2016, **369**, 131–137.
5 J. Homola, I. Koudela and S. S. Yee, *Sens. Actuators, B*, 1999, **54**, 16–24.
6 M. Lee, H. Jeon and S. Kim, *Nano Lett.*, 2015, **15**, 3358–3363.
7 D. Cai, Y. Lu, K. Lin, P. Wang and H. Ming, *Opt. Express*, 2008, **16**, 14597–14602.
8 H. R. Gwon and S. H. Lee, *Mater. Trans.*, 2010, **51**, 1150.
9 M. T. Flanagan and R. H. Pantell, *Electron. Lett.*, 1984, **20**, 968.
10 C. Nylander, B. Liedberg and T. Lind, *Sens. Actuators*, 1982, **3**, 79.
11 D. W. Huang, Y.-F. Ma, M. J. Sung and C.-P. Huang, *Opt. Eng.*, 2010, **49**, 054403.
12 M. Iga, A. Seki and K. Watanabe, *Sens. Actuators, B*, 2004, **101**, 368–372.
13 Y. Wang, S. Meng, Y. Liang, L. Li and W. Peng, *Photonic Sens.*, 2013, **3**, 202.
14 R. Jha and A. K. Sharma, *J. Opt. A: Pure Appl. Opt.*, 2009, **11**, 045502.
15 A. Shalabney and I. Abdulhalim, *Laser Photonics Rev.*, 2011, **5**, 571–606.
16 K. Roy, M. Padmanabhan, S. Goswami, T. P. Sai, G. Ramalingam, S. Raghavan and A. Ghosh, *Nat. Nanotechnol.*, 2013, **8**, 826–830.
17 C. Zhang, Z. Li, S. Z. Jiang, C. H. Li, S. C. Xu, J. Yu, Z. Li, M. H. Wang, A. H. Liu and B. Y. Man, *Sens. Actuators, B*, 2017, **251**, 127–133.
18 S. Huh, J. Park, Y. S. Kim, K. S. Kim, B. H. Hong and J. M. Nam, *ACS Nano*, 2011, **5**, 9799–9806.
19 L. Kang, J. Chu, H. Zhao, P. Xu and M. Sun, *J. Mater. Chem. C*, 2015, **3**, 9024–9037.
20 N. M. Das, S. Kumar and D. Bandyopadhyay, *Carbon*, 2017, **121**, 612–614.
21 Q. Ouyang, N. Panwar, S. Zeng, X. Wang, L. Jiang, X. Dinh, B. K. Tay, P. Coquet and K. Yong, *Monolayer $WS_2$ Enhanced High Sensitivity Plasmonic Biosensor based on Phase Modulation*, Optical Society of America, 2017, p. SM1C.4.
22 G. B. McGaughey, M. Gagné and A. K. Rappé, *J. Biol. Chem.*, 1998, **273**, 15458–15463.
23 S. Zeng, S. Hu, J. Xia, T. Anderson, X. Q. Dinh, X. M. Meng, P. Coquet and K. T. Yong, *Sens. Actuators, B*, 2015, **207**, 801–810.
24 A. K. Mishra, S. K. Mishra and R. K. Verma, *J. Phys. Chem. C*, 2016, **120**, 2893–2900.
25 Q. Ouyang, S. Zeng, L. Jiang, L. Hong, G. Xu, X. Q. Dinh, J. Qian, S. He, J. Qu, P. Coquet and K. T. Yong, *Sci. Rep.*, 2016, **6**, 28190.

26 G. B. McGaughey, M. Gagné and A. K. Rappé, *J. Biol. Chem.*, 1998, **273**, 15458–15463.
27 H. Fu, S. Zhang, H. Chen and J. Wang, *IEEE Sens. J.*, 2015, **15**, 5478–5482.
28 K. Tiwari, S. C. Sharma and N. Hozhabri, *J. Appl. Phys.*, 2015, **118**, 093105.
29 P. K. Maharana, P. Padhy and R. Jha, *IEEE Photonics Technol. Lett.*, 2013, **25**, 2156–2159.
30 P. Lecaruyer, M. Canva and J. Rolland, *Appl. Opt.*, 2007, **46**, 2361–2369.
31 C. Zhang, S. Z. Jiang, C. Yang, C. H. Li, Y. Y. Huo, X. Y. Liu, A. H. Liu, Q. Wei, S. S. Gao, X. G. Gao and B. Y. Man, *Sci. Rep.*, 2016, **6**, 25243.
32 X. Yu, H. Cai, W. Zhang, X. Li, N. Pan, Y. Luo, X. Wang and J. G. Hou, *ACS Nano*, 2011, **5**, 952–958.
33 X. Ling and J. Zhang, *J. Phys. Chem. C*, 2011, **115**, 2835–2840.
34 C. Zhang, S. Z. Jiang, Y. Y Huo, A. H. Liu, S. C. Xu, X. Y. Liu, Z. C. Sun, Y. Y. Xu, Z. Li and B. Y. Man, *Opt. Express*, 2015, **23**, 24811–24821.